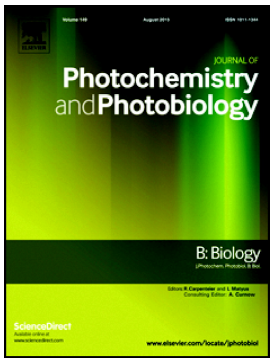

Imaging mitochondria and plasma membrane in live cells using solvatochromic styrylpyridines

Tarushyam Mukherjee, Aravintha Siva, Komal Bajaj, Virupakshi Soppina, Sriram Kanvah

PII: S1011-1344(19)31339-9

DOI: https://doi.org/10.1016/j.jphotobiol.2019.111732

Reference: JPB 111732

To appear in: *Journal of Photochemistry & Photobiology, B: Biology*

Received date: 7 October 2019

Revised date: 20 November 2019

Accepted date: 4 December 2019

Please cite this article as: T. Mukherjee, A. Siva, K. Bajaj, et al., Imaging mitochondria and plasma membrane in live cells using solvatochromic styrylpyridines, *Journal of Photochemistry & Photobiology, B: Biology*(2019), https://doi.org/10.1016/j.jphotobiol.2019.111732

Imaging Mitochondria and Plasma Membrane in Live Cells using Solvatochromic Styrylpyridines

Tarushyam Mukherjee[‡], Aravintha Siva[†], Komal Bajaj[‡], Virupakshi Soppina*[†] and Sriram Kanvah[‡#]*

[#‡•]Department of Chemistry, Indian Institute of Technology Gandhinagar, Palaj, Gandhinagar 382355, India. E-mail: sriram@iitgn.ac.in, kanvah@gatech.edu

[†•]Department of Biological Engineering, Indian Institute of Technology Gandhinagar Palaj Gandhinagar 382355 e-mail: vsoppina@iitgn.ac.in

Abstract

Investigating the dynamics of different biomolecules in the cellular milieu through microscopic imaging has gained paramount importance in the last decade. Continuous developments in the field of microscopy are paralleled by the design and synthesis of fluorophores that target specific compartments within a cell. In this study, we have synthesized four fluorescent styrene derivatives, a neutral styrylpridine, three cationic styrylpyridinium probes with and without cholesterol tether, and investigated for their absorption, emission, and cellular imaging properties. The fluorophores show solvatochromic emission attributed to intramolecular charge transfer from donor to acceptor with an emission range of 500-600 nm. The fluorescent cholesterol conjugate labels plasma membrane effectively while the fluorophores devoid of the cholesterol tether label mitochondria. Cholesterol conjugate also shows strong interaction with liposome membrane. Furthermore, the fluorophores were also used to track the mitochondria in live cells with high specificity. Cell viability assay showed overall non-toxic nature of the probes even at high concentrations. Through sidearm modifications, keeping the fluorescent core intact, we successfully targeted specific subcellular compartments of neuronal (N2a) and non-neuronal (HeLa) mammalian cell lines. This strategy of using a single molecular scaffold with subtle substitutions could be ideal in generating a variety of fluorophores targeting other subcellular compartments.

Keywords

Fluorescent Sterols, Intramolecular Charge Transfer, Mitochondrial Imaging, Plasma membrane staining, Styrlpyridines.

Introduction

Targeted imaging of sub-cellular organelles is of paramount importance in cell biology and has triggered numerous investigations towards the design of various fluorophores[1-5]. The basic unit of life, a cell, is an intricately organized and highly dyramic entity, where the many organelles carry out specialized functions inside and yet regularly interact with one another. To get the accurate details of the cellular activities, visualization of these organelles becomes necessary. This necessity steered the research towards fluorophore-based targeted imaging that gives us visual evidence of the cellular world. For this purpose, Donor-π-Acceptor based fluorescent organic molecules offer several tunable design strategies. A particularly exciting scaffold based on styrylpyridine, offering strong environmental sensitivity was extensively investigated for various applications including, DNA intercalation or groove binding[6-9], analyte detection [10-12], imaging of plasma membrane[13] and mitochondria [14-16], histological staining [17, 18], investigation of norepinephrine transportation[19, 20] formations of supramolecular assemblies [21-26] and organic electronic applications[27-30]. In the current study, we systematically investigate the utility of styrylpyridine and its derivatives to image cellular compartments such as the plasma membrane and mitochondria. The plasma membrane apart from maintaining cell integrity plays a vital role in various other processes such as signal transduction, cell differentiation, and cell fusion. Thus, designing membrane probes that can effectively label the plasma membrane might be beneficial for a better understanding of the cellular structure. A typical probe must have red-emission to enable penetration depth, cellular membrane compatibility and preferably possess a suitable recognition moiety. For this purpose, we utilized styrylpyridine as an extrinsic fluorophore linked to the cholesterol moiety to investigate cellular imaging. Cholesterol is an integral member of the mammalian cell membrane, and it provides structural stability to the cell. Hence, targeting cell membrane or cellular processes has been achieved through the tagging of the probe with cholesterol[31, 32]. Various reporter molecules such as NBD[33], Bodipy[32, 34], pyrene[35], Dansyl[36], and

others were conjugated to cholesterol and were used to study cellular processes such as trafficking, model membrane studies, and biomolecular interactions[37].

Furthermore, among the various units of cell organelles, mitochondria, the powerhouse of the cells, always hold particular importance due to its complex functionality that regulates cellular physiological states[38, 39]. Consequently, monitoring of mitochondrial processes through the use of fluorophores received significant attention [14, 40-42]. In this work, we utilize a single fluorescent core to achieve targeted imaging of the plasma membrane and mitochondria. In short, we synthesized four styrylpyridines (Scheme-1): the neutral styrylpyridine **1**, cationic methyl pyridinium derivative **2**, hydroxyl propyl pyridinium derivative **3**, and novel pyridinium-cholesterol conjugate **4**. The newer fluorescent cholesterol conjugate **4** exhibits large Stokes' shift with excitation and emission in the visible region and shows high specificity to the plasma membrane with no cytotoxicity. A comparison with existing cholesterol conjugates is given in Table- S1. Interestingly the styrylpyridines **1-3** devoid of the cholesterol linker stain the mitochondria in green to red regions, while the pyridinium cholesterol conjugate labels the cell membrane. We have also demonstrated the ability to track live mitochondrial movement and mitochondrial events such as fusion, fission with the help of our mitochondrial specific styrene probes. The results of absorption, emission, and cellular imaging studies are presented in the following sections.

Experimental Methods

All the necessary chemicals and reagents required for the synthesis of the probes were purchased from Aldrich, Alfa Aeser, TCI Chemicals, Avra Synthesis, or SD Fine-Chem. The synthesized samples were characterized using ^{1}H and ^{13}C NMR (Bruker Advance III-500 MHz) in chloroform-D or dimethyl sulphoxide (D_6) solvents. The absorption studies were performed on Analytik Jena Specord 210 instrument, and the steady-state and the fluorescence studies were measured using Horiba Jobin Yvon Fluorolog-3 spectrofluorimeter with a slit width of 2 nm. The sample concentrations used for the fluorescence studies are in the order of 10 μM. The excitation wavelength for recording the emission spectra is typically kept at the absorption maxima of the samples under investigation. Mass spectral data is recorded using Water Synapt G2S ESI Q-ToF mass spectrometer.

Model membrane preparation

DPPC model membrane was prepared by a solvent evaporation method. DPPC lipid was dissolved in chloroform-methanol 2:1 (v/v) at the desired molar ratio, and after that, the solvent layer was dissolved under reduced pressure. The dried lipid layer was hydrated soon after the solvent layer was evaporated by the addition of triple distilled water and kept in 55°-60° C to form final vesicles. The required amount of probe (0.4 mM) was incorporated into the lipid layer in the chloroform-methanol mixture. Imaging of model membrane was performed on a Leica Laser Scanning Confocal microscope (TCS SP8) equipped with HyD and PMT detectors using a 458 nm laser.

Plasmids

Plasmids coding for fluorescently-tagged subcellular organelle specific markers such as Mito-ECFP and Mito-DsRed were generated by sub-cloning into ECFP-N1 and DsRed-N1 plasmids and used for labeling the mitochondria. ECFP-MEM was generated likewise by sub-cloning into ECFP-C1 to label the plasma membrane. KDEL-BFP and LAMP1-YFP were also generated similarly for the labeling of endoplasmic reticulum and lysosome respectively.

Cell culture and live-cell imaging:

HeLa and Cos-7 cells were grown in DMEM (Gibco) supplemented with 10% FBS (Gibco) and 2 mM GlutaMAX (Gibco) at 37° C in a humidified environment with 5% CO_2. EMEM (Gibco) was used in the place of DMEM for culturing N2a cells. For live-cell imaging studies, 1.5 x 10^5 cells were grown on glass-bottom dishes. These cells were subsequently transfected with 1 µg of plasmid DNA using TurboFect transfection reagent (Thermo Scientific) and incubated overnight. On the following day, cells were further treated by adding 2 µl of the probe from 1 mM stock (prepared in DMSO) to 2 ml of DMEM and incubated for 10 min at 37°C and washed three times in HEPES buffer (pH 7.4) before imaging under the microscope. Live-cell imaging was performed on a Leica Laser Scanning Confocal microscope (TCS SP8) at 37°C temperature in the presence of 5% CO_2. Images were obtained using 405 nm, 458 nm and 561 nm lasers (for the fluorescent proteins: 405 nm and 561 nm lasers used for Mito-CFP, ECFP-MEM, and Mito-DsRed respectively; wherein for the styrene-1 we have used 405 nm and styrene-2 to styrene-4: 458 nm laser) and the emission signals were collected using HyD and PMT detector.

Mitochondrial tracking experiments live-cell imaging was performed in epifluorescence mode using a Nikon inverted microscope (Nikon Eclipse Ti2, Japan) equipped with $37^{O}C$ with 5% CO_2 EMCCD camera (Andor iXon 897Ultra, USA). Images were acquired at ten frames/sec using Nikon software (NIS element AR, Japan).

Mitochondrial membrane potential change Cells were seeded to the 35 mm glass-bottomed live-cell dishes at a density of 1.5 × 105 cells per dish in culture medium. After 24 h, cells were treated with 20 μM CCCP for 20 min and incubated with 1 μM probe before live-cell imaging using Laser Scanning Confocal microscopy (Leica SPI8).

Cell Viability Assay

MTT assay was performed to calculate the toxicity of the probe in mammalian cells. Five thousand HeLa cells were seeded per well and grown in 96- well plates. After 24 h of seeding, the cells were treated with different concentrations (0.25, 0.5, 1, 2, 4, 8, and 10 μM) of the probes respectively and incubated for 24 h. The cells that served as the negative control containing respective concentration (v/v) of DMSO alone (without any probe) were replenished with fresh media. After the treatment duration, the media was aspirated from all the wells and incubated further with 0.5 mg/mL of MTT for 4 h. Media containing the MTT was then removed after which, DMSO was added to solubilise the formazan. The absorbance values were recorded using BioTek SYNERGYH1 plate reader at 570 nm. Absorbance values of cells treated with the probes were normalized against the untreated cells (negative control). The percentage cell viability was calculated with the help of the negative control as reference, where the cells were treated with solvent (DMSO) alone. Finally, the percentage cell viability is plotted against probe concentration as mean ± SD. The results presented are an average of three independent sets of experiments.

Data Analysis

Analysis and quantification of co-localization were performed using ImageJ software (nih.gov). The overlap coefficient and Pearson correlation coefficient (PCC) were evaluated by using the co-localization finder plugin of the same software. Background fluorescence was subtracted from this maximum value for the respective filter, and then the pixel intensity comparisons were carried out.

Mitochondrial tracking Individual mitochondria were tracked frame-by-frame using the custom-written plugin in ImageJ (nih.gov), and graphs were plotted in Origin 9.1 (Origin Lab).

Results and Discussion

Synthesis

The styryl probes (**1-4**) were prepared as per the scheme-1 given below. 4-picoline was condensed with dimethylamino benzaldehyde to yield the neutral styrene **1**. Methylation of **1** with methyl iodide produced styrene **2,** and the reaction of **1** with 3-bromopropanol yielded styrene **3** bearing a 3-carbon linker with a hydroxyl terminus. Reaction with 3-bromopropyl cholesteryl formate, prepared by using cholesteryl chloroformate and 3-bromopropanol[43] with styrene **1** yielded cholesterol conjugated styrene **4**. Except styrene **1**, the other styrenes **2-4** contain a single cationic charge that facilitated their solubility in aqueous media. The synthetic procedures and the characterization spectral data are given in the supporting information.

Absorption and emission studies

The absorption and emission data of the styrenes **1-4** are summarized in Table-1. Styrene **1** bearing a dimethylamine donor and pyridine acceptor absorbs at ~370 nm in non-polar dioxane. Styrene, **2**, containing pyridinium group shows significant bathochromic shifts with absorption maxima at 463 nm. The wavelength shifts are a result of extended conjugation owing to the presence of a robust electron-withdrawing pyridinium group. Styrene **3** with a hydroxypropyl unit and styrene **4** having a cholesterol moiety does not affect the absorption maxima [Fig 1a]. The molecules show moderate solvatochromic shifts with increasing solvent polarity. Styrene **1** absorbs at 370 nm in dioxane and shows absorption at 379 nm in polar DMSO. Styrenes **2-4** [Fig 1b and Fig S1] also show moderate solvatochromic effects with an increase in solvent polarity: 463 to 471 nm for **2**, 463 to 475 nm for **3** and 464 nm to 477 nm for **4**. For cationic styrenes **2-4**, the absorption spectra are broad and show a hypsochromic shift in water. The broad absorption spectra in water could be due to weaker water solubility, and the hypsochromic shift is attributed to charge stabilization in water [12, 44].

Table 1: Absorption and emission of styrenes **1-4** in homogeneous solvents.

Solvent	1		2		3		4	
	λ_a (nm)	λ_f (nm)	λ_a (nm)	λ_f (nm)	λ_a (nm)	λ_f (nm)	λ_a (nm)	λ_f (nm)
Dioxane	370	445	465	555	463	570	465	565
THF	372	485	470	595	474	594	470	595
DMSO	380	495	470	617	475	628	478	615
DMF	375	483	470	615	475	617	478	610
CH_3CN	370	485	470	615	473	616	478	610
CH_3OH	377	500	476	605	480	606	483	606
H_2O	-	522	450	610	455	615	455	610

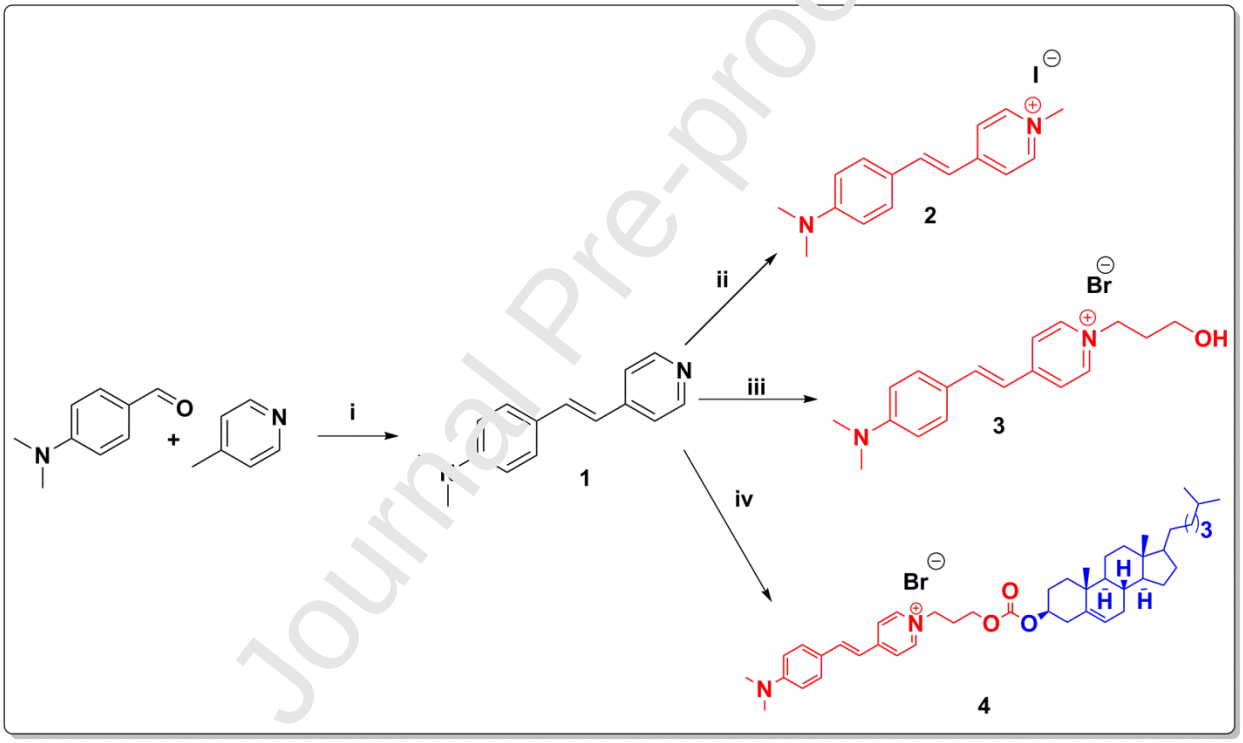

Scheme 1. Synthetic strategy for the Styrenes 1-4. Reaction Conditions: (i) KOH, 125°C, 8 h; (ii) Ethanol, 100°C, 8-9 h; (iii) 3-bromopropanol, acetonitrile, 100°C, 16 h; (iv) 3-bromopropyl cholesterylformate, triethylamine, dry DCM, 0°C, 12 h.

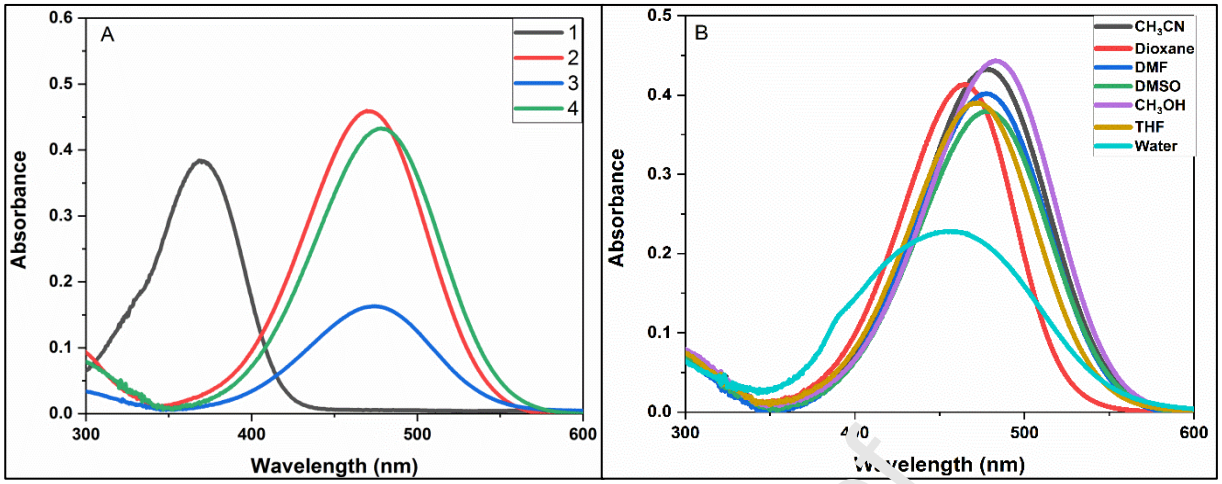

Fig. 1. Absorption spectra of styrenes **1-4** in (A) acetonitrile and absorption spectra of (B) styrene **4** in different solvents.

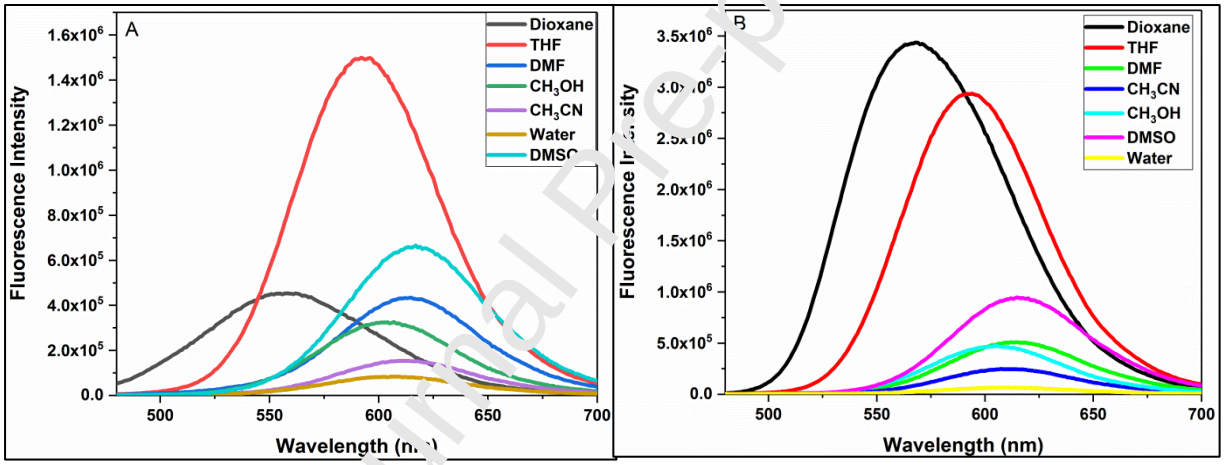

Fig. 2. Emission spectra of (A) styrene **2** and (B) styrene **4** in different solvents

Analogous to the absorption data, the emission of neutral styrene **1** significantly differs from the cationic fluorophores **2-4**. Neutral styrene **1** emits at 445 nm in dioxane, but cationic compounds show emission at 554-570 nm regions. Solvent polarity has a strong effect on the emission of the styrenes. Upon increasing the solvent polarity, gradual emission changes were obtained with an overall bathochromic shift of 50 nm (styrene **1**) from dioxane to dimethylsulfoxide [Fig S2a]. The bathochromic shifts observed for styrenes **2-4** are similar to the neutral derivative with shifts in the range of 50 -65 nm [Fig 2 and Fig S2b], and the shifts are attributed to the charge stabilization in polar solvents[45]. On the other hand, substitution with hydroxyl alkyl or cholesteryl tethers does not impact the emission behavior as compared to styrene **2**.

Interaction with model membrane

Liposomes possess long-chain hydrophobic fatty acids and mimic the plasma membrane *in vitro*[46, 47]. The cholesterol tether can contribute to the enhanced hydrophobicity and target the membrane easily. Considering the inherent property, we have investigated the spectroscopic behavior of the cholesterol-conjugate **4** in the liposome membrane to evaluate its membrane binding characteristics. Styrene **4** exhibited ~40 fold increment (at 570 nm) in fluorescence intensity [Fig 3A] in DPPC (dipalmitoylphosphatidylcholine) model membrane system along with ~40 nm blue shift in the emission wavelength. This emission change is an indication of probe-liposome interaction[48]. We presume that the cholesterol 'head group' in probe **4** is anchoring the molecule into the membrane, and the remainder fluorescent core lies outside. Styrene **4** is also able to sense the phase transition temperature of the membrane since the change in the fluorescent intensity decrement is evident from the spectral behavior[48] [Fig S3]. To further validate the specificity, we imaged the liposomes using laser scanning confocal microscopy and probe (styrene **4**) showed strong colocalization with liposome membrane [Fig 3B]. The cumulative spectroscopic and microscopic response has thus inspired us to study cellular imaging for the plasma membrane.

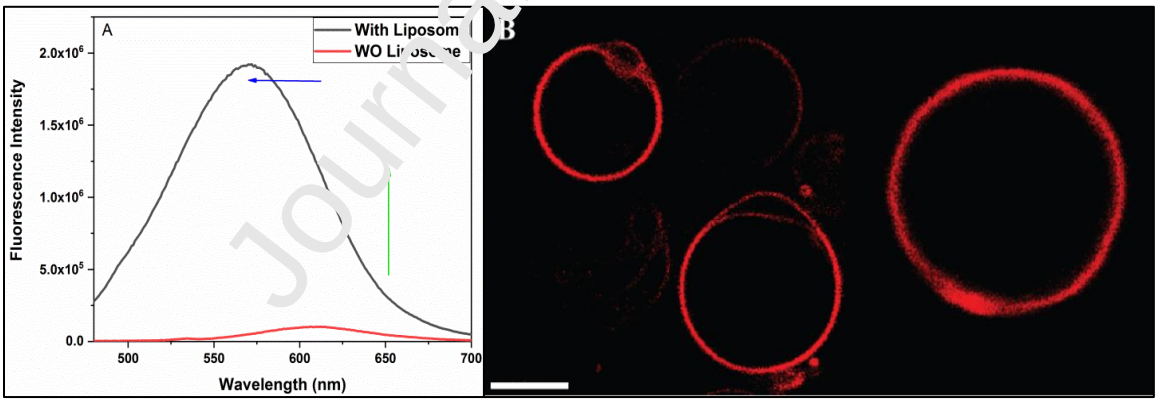

Fig. 3: Interaction of styrene-4 with *in vitro* model membrane: (A) Emission behavior of styrene **4** in water and model membrane (DPPC) [Green and blue lines indicate the intensity enhancement and blue shift of the styrene **4** after binding to model membrane], (B) Confocal microscopy images of DPPC membrane tagged with styrene **4**; scale bar: 5 µm.

Subcellular localization of the styrene probes:

Styrene probes label mitochondria and cell membrane in HeLa cells

Styrylpyridine and its derivatives have been explored for use in various cellular processes and are also known for organelle-specific imaging[13, 14, 49]. Here, we aimed to label specific subcellular compartments using fluorescent probes containing a single styrylpyridine core. Generally, the cationic pyridinium core of styrenes enables better electrostatic interaction with the mitochondrial membrane[39, 50]. To explore their specificity and competence of subcellular localization, we performed fluorescence live-cell imaging using microscopy. In live HeLa cells, all four styrenes efficiently crossed the plasma membrane within 10 min of incubation and showed intense subcellular distribution. Styrenes **1-3** show dynamic long thread-like structures that are uniformly distributed in the cytoplasm resembling mitochondrial localization, while styrene **4** strongly labeled the cell periphery. The subcellular localization was further confirmed by incubating the probes with cells expressing FP (fluorescent protein)-tagged organelle-specific markers. The incubation of probes **1**, **2** and **3** with HeLa cells expressing FP-tagged mitochondria specific markers, Mito-DsRed and Mito-ECFP, showed robust co-localization with the mitochondrial compartment (Fig 4 A-L). As compared to styrene **1** (PCC: 0.18), the styrenes **2** and **3** showed better mitochondrial specificity (PCC: 0.56 and 0.78, respectively) with a high signal-to-noise ratio. Furthermore, we have also expressed other cell organelle specific fluorescent markers. We transfected the Cos-7 cells with BFP-KDEL (Endoplasmic reticulum marker) and LAMP1-YFP (Lysosome marker) plasmids before imaging. The observed morphological pattern: mesh-like network of ER and circular structures of lysosome is distinct from the thread-like mitochondrial structures obtained with styrenes **2** and **3** [Fig. S4]. Styrene **4** showed strong co-localization (PCC: 0.52) with plasma membrane labeled with ECFP-MEM (Fig. 4 M-P), FP-tagged plasma membrane-specific marker. We also analyzed the intensity profile of various cellular regions and compared the signal intensity of both compound and marker channels (Fig. 4 D, H, L, and P). The results for styrenes **2** and **3** are consistent with the previous findings of the cationic pyridinium derivative's capability to exploit the electrochemical potential of the mitochondrial membrane and label mitochondria specifically *in vivo* [51, 52].

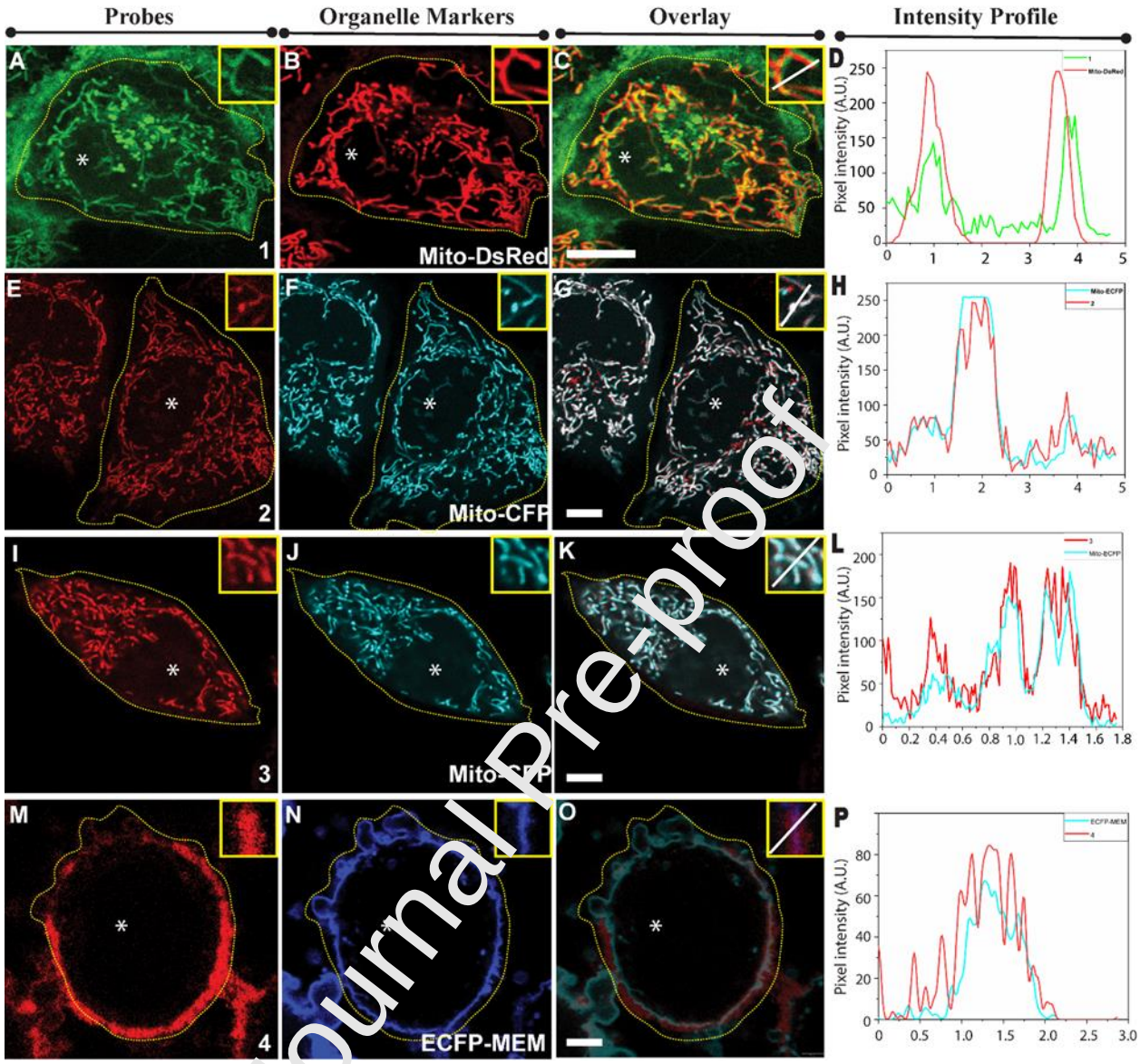

Fig. 4. Labeling of subcellular compartments with styrenes in HeLa cells. Styrenes (**1-4**, extreme left panel; 1 µM of each styrene) were incubated with HeLa cells expressing fluorescent protein (FP)-tagged organelle-specific markers (second panel from left) and overlaid (third panel from left). Representative images of cells incubated with (A-C) Styrene **1** (E-G) Styrene **2** (I-K) Styrene **3**, and (M-O) Styrene **4**. (D, H, L and P) represent the intensity profile of line drawn in the ROI shown in inset images of respective styrenes (extreme right panel). Dotted yellow lines indicate the outline of transfected cells; white asterisks indicate nuclei. (scale bars, 10 µm).

Being a neutral derivative and owing to lower solubility, styrene **1** show high background noise in the emission signal (Fig. 4 A). On the other hand, the presence of cholesterol moiety in styrene **4** provides extra leverage to target the plasma membrane by interacting with the lipid and cholesterol-rich domains of the mammalian cell membrane making styrene **4** a lucrative probe. Together the data suggest that the importance of sidearm modifications of the single fluorescent core in targeting different cellular compartments.

Styrenes label mitochondria and cell membrane in N2a cells

For assessing the labeling ability of the styrenes in other cell types, we also performed live-cell imaging with the N2a cell line (neuroblastoma cells). Although the foundational architecture is the same as non-neuronal cells, neurons exhibit unique and specialized functionalities. Thus imaging the various compartments hold promise in elucidating minuscule details of the neurons. The results of the co-localization assay showed that styrenes **2** and **3** efficiently labeled the mitochondria, while styrene **4** show robust localization in the plasma membrane, corroborating our earlier observations in HeLa cells [Fig 5]. Apart from calculating the Pearson coefficient, we have also analyzed the pixel intensities from each compound and marker channels, and data indicated a healthy overlapping pattern [Fig 5].

Styrene probes are not cytotoxic

The suitability of a probe for its use in living cells can be ascertained by examining its cellular toxicity. In this context, the cytotoxicity of the synthesized styrenes was assessed by a 3-(4,5-dimethylthiazol-2-yl) 2,5-diphenyltetrazolium bromide (MTT) assay. No relevant signs of cytotoxicity were observed even while working at high concentrations (10 μM) over 24 h for all styryl probes [Fig 6]. This further strengthens our claim to use them as cellular probes for labeling subcellular compartments in live and fixed cells. Besides, the effect of the solvent used for the imaging experiments was also found to be non-significant in toxicity experiment.

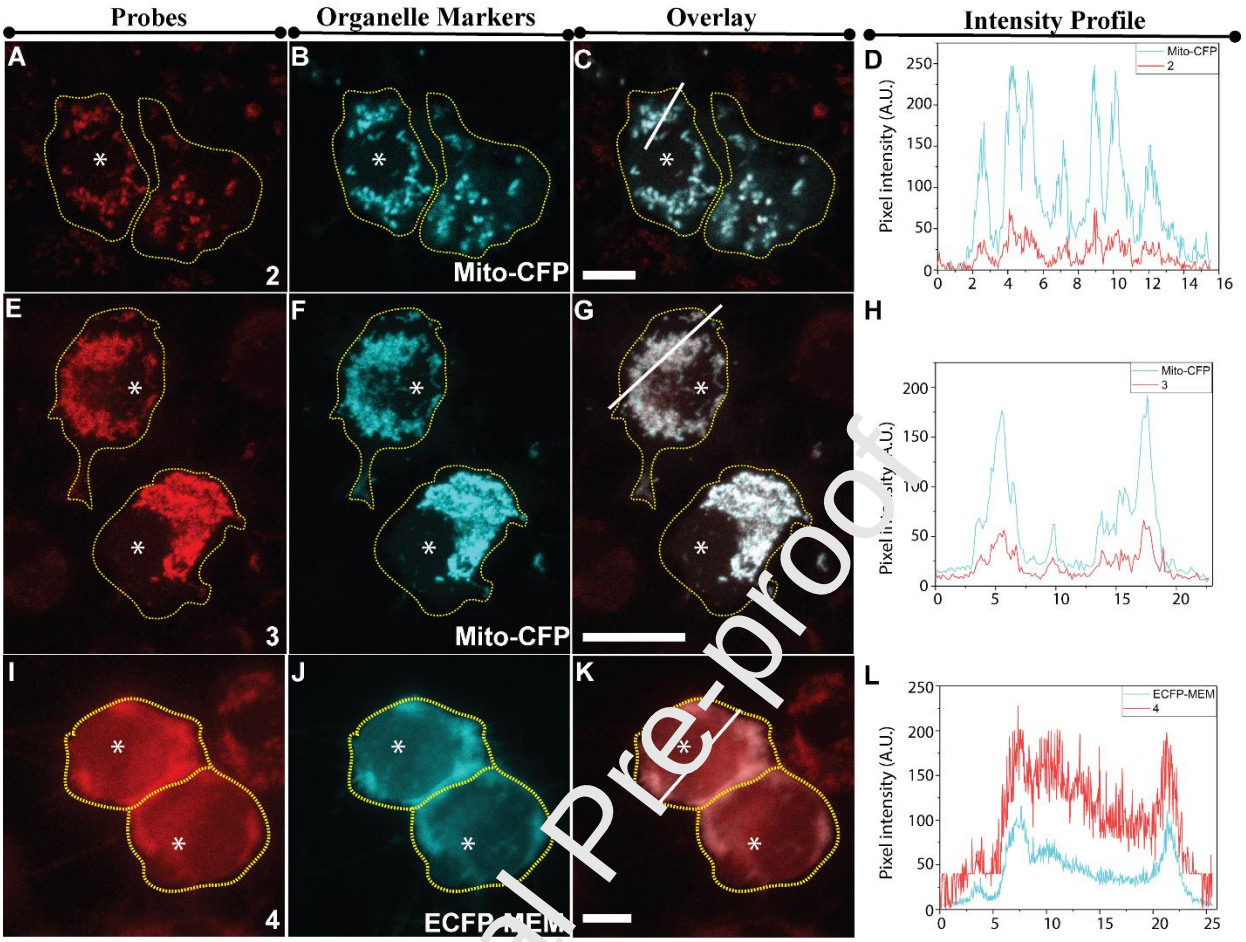

Fig. 5. Labeling of subcellular compartments with styrene probes in N2a cells. Styrenes (**2-4** – extreme left panel; 1 µM of each styrene) incubated with cells expressing fluorescent protein (FP)-tagged organelle-specific markers (second panel from left) and overlaid (third panel from left). Representative images of cells incubated with (A-C) Styrene **2** (E-G) Styrene **3** and (I-L) Styrene **4**. (D, H, and L) represent the intensity profile of line drawn in the images of respective styrenes (extreme right panel). Dotted yellow lines indicate the outline of transfected cells; white asterisks indicate nuclei. (scale bars, 10 µm).

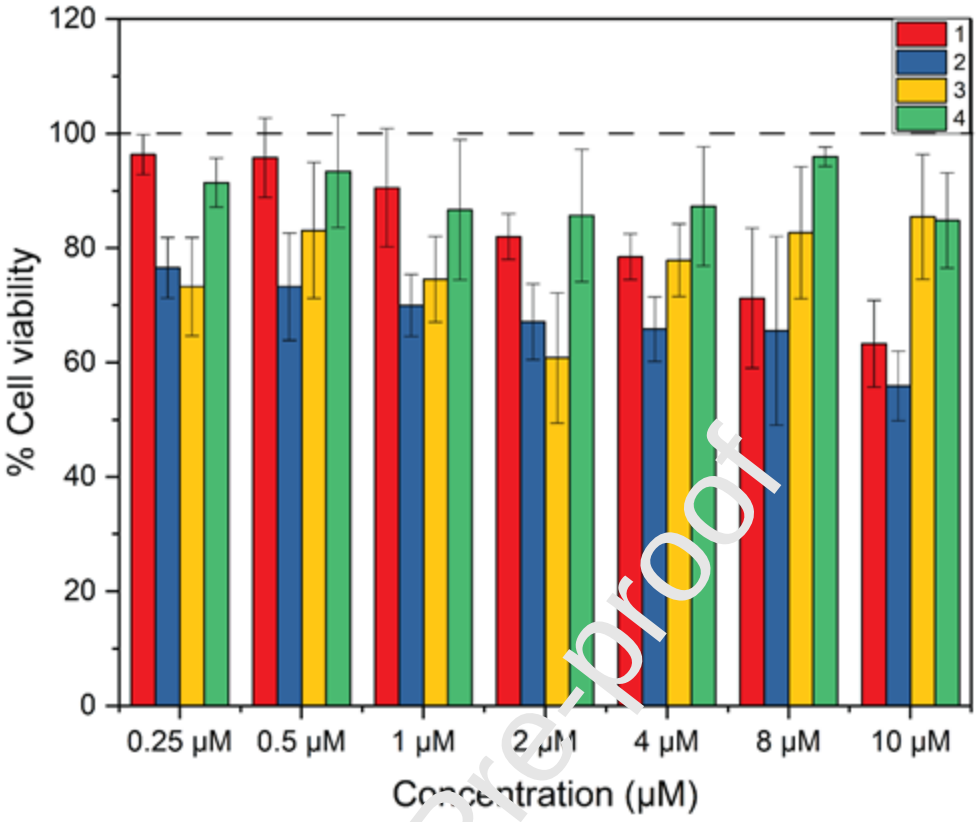

Fig. 6. Cell viability assay of styrenes **1-4** investigated using the MTT assay; the dotted line signifies the negative control where the cells were not treated with any probes.

Styrenes for live mitochondrial tracking in mammalian cells.

Mitochondria are highly motile and dynamic organelles. Their motility affects their functionality in terms of cell division, development, and overall cellular growth. Interestingly they exhibit different behavior at the onset of altered physiological and metabolic states that eventually lead to several diseases such as Alzheimer's, Parkinson's, and cancer[53, 54]. Hence visualizing these differences over a periodical change of time is pertinent through tracking them with specific probes. The live-cell tracking of mitochondria using external fluorophores requires the probe's specificity towards mitochondrial membrane potential, low toxicity, high signal-to-noise ratio, and high photostability[54]. By these parameters, we herein, track the mitochondrial movement, mitochondrial fission and fusion events with the help of our mitochondria selective styrenes **2** and **3** [Fig 7 A and B, SI movie-1 and movie-2]**.** We were able to trace the mitochondrial dynamics, such as microtubule-based bidirectional motion due to simultaneous presence and activity of plus- and minus end-directed microtubule-based motor proteins of kinesins and

dyneins respectively on the mitochondrial membrane[55, 56], Representative tracks of mitochondrial tracks for **2** and **3** are shown in Figure 8.

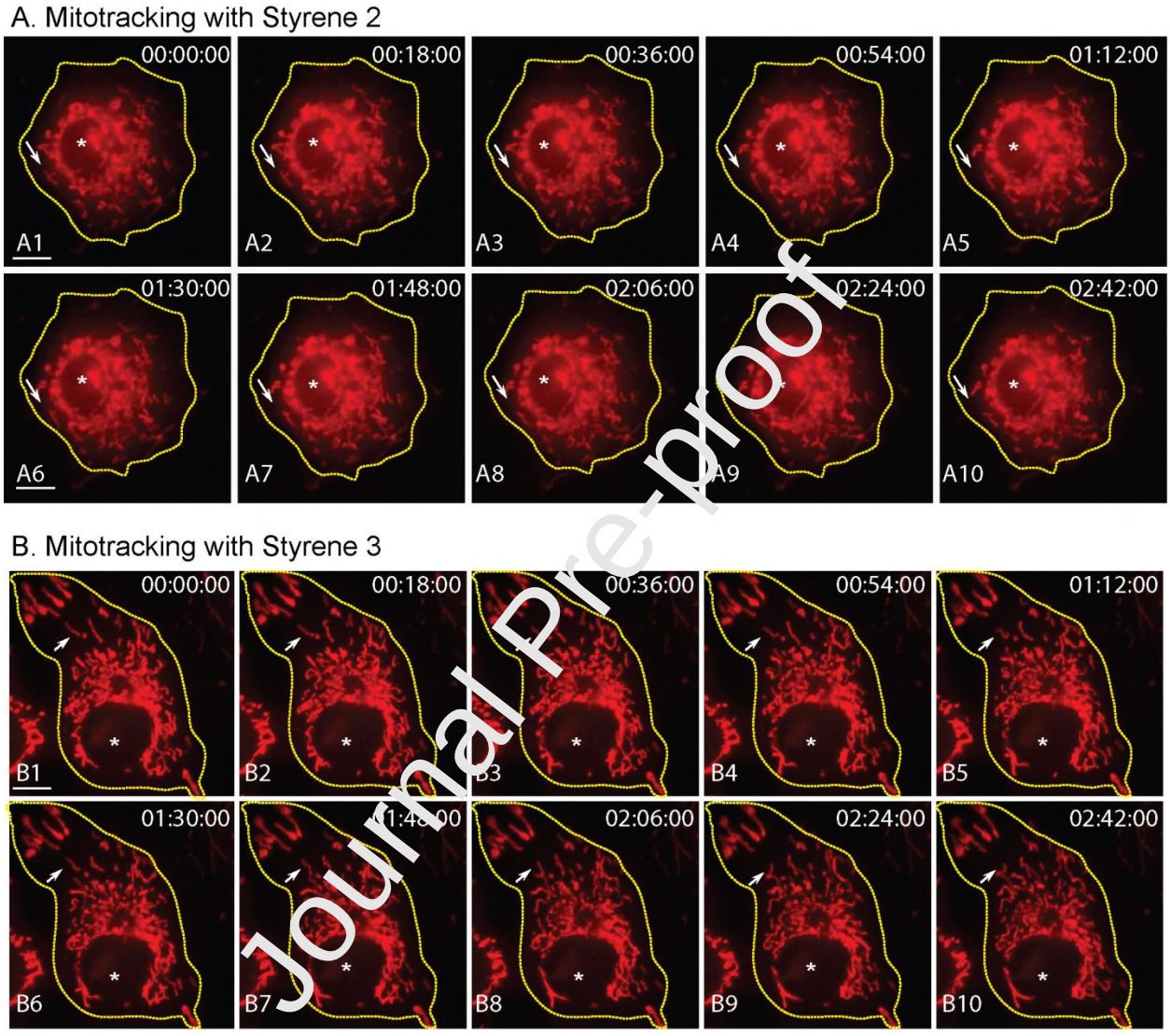

Fig. 7. Live mitochondria tracking in mammalian cells: (A1-A10) A montage of a representative cell treated with 1 μM styrene-2 showing live mitochondrial motion at different points. (B1-B10) A montage of a representative cell treated with 1 μM styrene-**3** showing live mitochondrial motion at different time points. Dotted yellow lines indicate the outline of cells treated with styrene probe; white asterisks indicate nuclei; white arrow indicates the movement of single mitochondria over time. (scale bars, 10 μm).

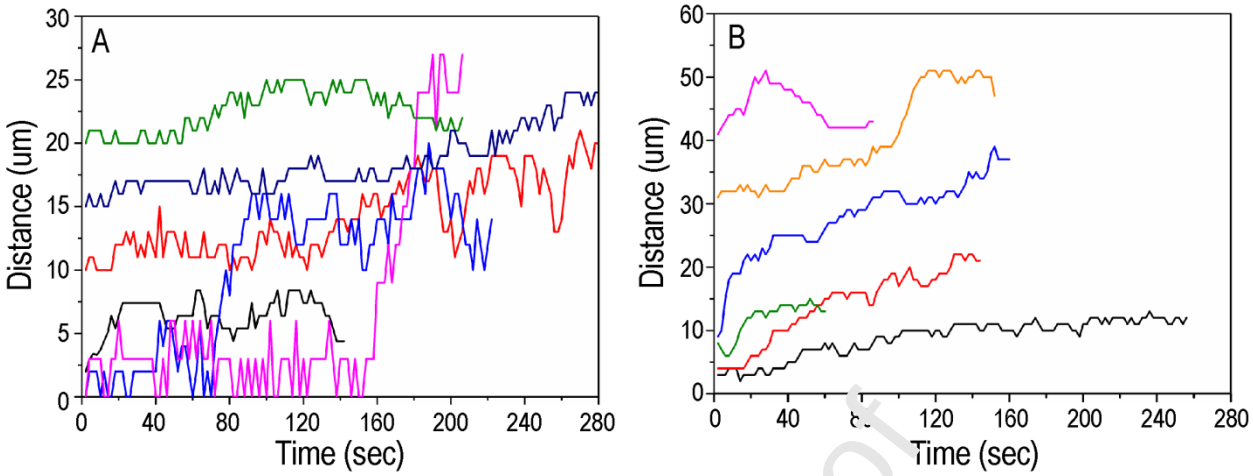

Fig 8: High-resolution live-cell tracking of mitochondria motion using Styrenes: Mitochondria were fluorescently labeled with Styrene probes and used for tracking their dynamics in live cells. Representative tracks of typical bidirectional motion of mitochondria in cells labeled with A) Styrene **2** and B) Styrene **3**.

Styrenes are sensitive to mitochondrial membrane potential

To test the sensitivity of the fluorophores to mitochondrial membrane potential, the cells were treated with CCCP (Carbonyl cyanide *m*-chlorophenyl hydrazine), a mitochondrial membrane potential uncoupler. At the onset of disturbed membrane potential, styrene **3** doesn't show specific mitochondrial binding as is evident from the fluorescence signal throughout the cells (Fig 9). Thus the binding of the fluorophore is dependent on the membrane potential and its electrostatic mode of interaction.

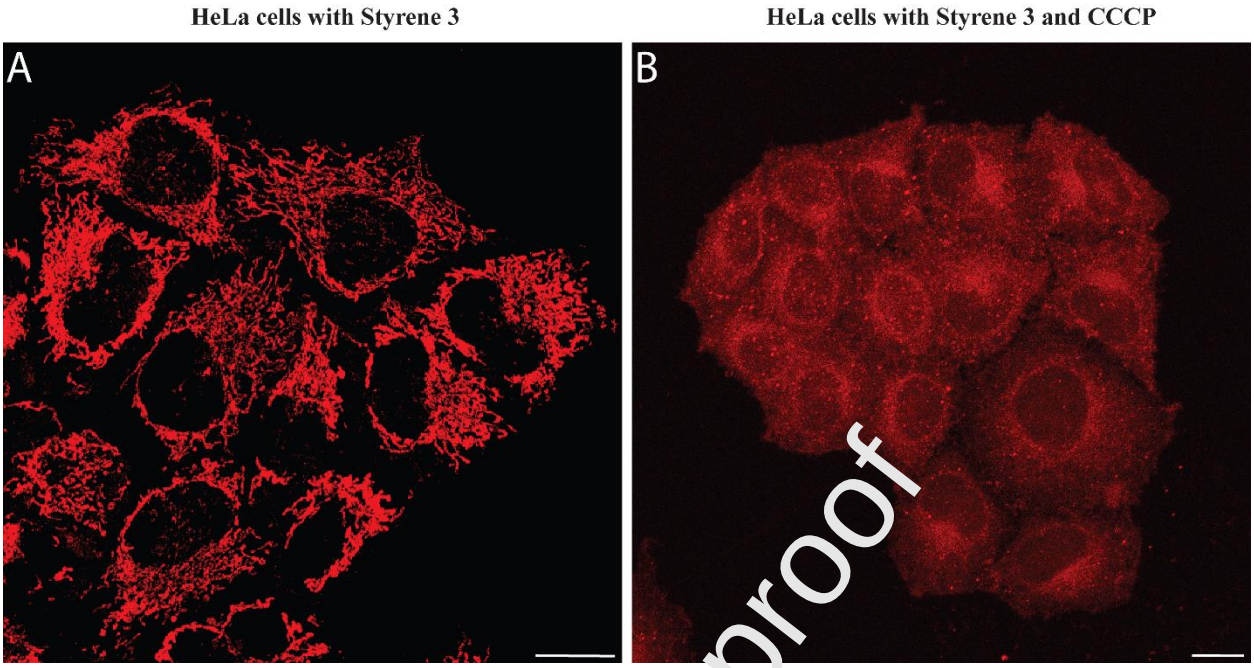

Fig 9: Styrene binding to mitochondria is membrane potential sensitive: (A) HeLa cells treated with styrene **3** and (B) HeLa cells incubated with **3** in presence of CCCP. Scale: 5 µM.

Conclusion

In summary, we demonstrated the solvatochromic behavior and cellular localization of four styrene probes in non-neuronal and neuronal cell lines. Mitochondria- specific localization was observed for cationic styrenes **2** and **3**, whereas the styrene **1** had a low signal to noise ratio in its ability to stain mitochondria. Furthermore, we have also demonstrated tracking of the live mitochondrial movements in cells and revealed that our dyes are sensitive to monitor live mitochondrial dynamics in real-time. Styrene **4** with pendant cholesterol successfully targets the plasma membrane and shows strong interaction with liposomes. We expect this work might give a holistic approach to the scientific community towards designing various organelle-specific probes keeping a single fluorescent core, which in turn enables us to work more efficiently in multiple optical windows.

Supporting Information: Absorption, emission, and synthetic characterization data are provided.

Conflicts of Interest: A provisional Indian patent aApplication (IP 201921044149) was filed.

Acknowledgments

Authors (SK, TM, KB) acknowledge funding support from SERB, Govt. of India (CRG/2018/004020). VS, AS acknowledges DBT (Grant No.: BT/PR15214/BRB/10/1449/2015 and BT/RLF/Re-entry/45/2015) and DST-SERB (Grant No.: ECR/2016/000913) for financial support. IIT Gandhinagar for general infrastructural support is also acknowledged.

References

[1] E. Kozma, P. Kele, Fluorogenic probes for super-resolution microscopy, Org. Biomol. Chem., 17 (2019) 215-233.
[2] L. Truong, A.R. Ferré-D'Amaré, From fluorescent proteins to fluorogenic RNAs: Tools for imaging cellular macromolecules, Protein Science, 28 (2019) 1374-1386..
[3] H. Zhu, J. Fan, J. Du, X. Peng, Fluorescent Probes for Sensing and Imaging within Specific Cellular Organelles, Acc. Chem. Res., 49 (2016) 2115-2126.
[4] W. Xu, Z. Zeng, J.-H. Jiang, Y.-T. Chang, L. Yuan, Discerning the Chemistry in Individual Organelles with Small-Molecule Fluorescent Probes, Angew. Chem. Int. Ed., 55 (2016) 13658-13699.
[5] X.-P. He, Y. Zang, T.D. James, J. Li, G.-R. Chen, J. Xie, Fluorescent glycoprobes: a sweet addition for improved sensing, Chemical Commun., 53 (2017) 82-90.
[6] D.V. Berdnikova, N.I. Sosnin, O.A. Fedorova, H. Ihmels, Governing the DNA-binding mode of styryl dyes by the length of their alkyl substituents – from intercalation to major groove binding, Org. Biomol. Chem., 16 (2018) 545-554.
[7] B. Kumari, A. Yadav, S.P. Pany, P.I. Pradeepkumar, S. Kanvah, Cationic red emitting fluorophore: A light up NIR fluorescent probe for G4-DNA, J. Photochem. Photobiol., B, 190 (2019) 128-136.
[8] C. Allain, F. Schmidt, R. Lartia, G. Bordeau, C. Fiorini-Debuisschert, F. Charra, P. Tauc, M.P. Teulade-Fichou, Vinyl-Pyridinium Triphenylamines: Novel Far-Red Emitters with High Photostability and Two-Photon Absorption Properties for Staining DNA, ChemBioChem, 8 (2007) 424-433.
[9] B. Dumat, G. Bordeau, E. Faurel-Paul, F. Mahuteau-Betzer, N. Saettel, G. Metge, C.l. Fiorini-Debuisschert, F. Charra, M.-P. Teulade-Fichou, DNA switches on the two-photon efficiency of an ultrabright triphenylamine fluorescent probe specific of AT regions, J. Am. Chem. Soc., 135 (2013) 12697-12706.
[10] R. Badugu, J.R. Lakowicz, C.D. Geddes, Enhanced Fluorescence Cyanide Detection at Physiologically Lethal Levels: Reduced ICT-Based Signal Transduction, J. Am. Chem. Soc., 127 (2005) 3635-3641.
[11] A.K. Vasu, S. Kanvah, Red-emitting cationic fluorophore as a probe for anionic surfactants, Dyes Pigm., 142 (2017) 230-236.
[12] P. Jana, M. Radhakrishna, S. Khatua, S. Kanvah, A "turn-off" red-emitting fluorophore for nanomolar detection of heparin, Phys. Chem. Chem. Phys., 20 (2018) 13263-13270.
[13] L. Guo, R. Zhang, Y. Sun, M. Tian, G. Zhang, R. Feng, X. Li, X. Yu, X. He, Styrylpyridine salts-based red emissive two-photon turn-on probe for imaging the plasma membrane in living cells and tissues, Analyst, 141 (2016) 3228-3232.
[14] C.S. Abeywickrama, K.J. Wijesinghe, R.V. Stahelin, Y. Pang, Bright red-emitting highly reliable styryl probe with large stokes shift for visualizing mitochondria in live cells under wash-free conditions, Sens. Act. B: Chem., 285 (2019) 76-83.
[15] L. Yang, J.-Y. Niu, R. Sun, Y.-J. Xu, J.-F. Ge, Rosamine with pyronine-pyridinium skeleton: unique mitochondrial targetable structure for fluorescent probes, Analyst, 143 (2018) 1813-1819.

[16] Z. Ding, M. Tian, L. Guo, Z.-q. Liu, X. Yu, Modulate the structures and photophysical properties of pyrene-based far-red fluorescent cationic dyes by regio-effect, Sens. Act. B: Chem., 276 (2018) 331-339.
[17] L. Magrassi, D. Purves, J.W. Lichtman, Fluorescent probes that stain living nerve terminals, J. Neuroscience, 7 (1987) 1207-1214.
[18] R. Krieg, A. Eitner, W. Günther, C. Schürer, J. Lindenau, K.J. Halbhuber, N, N-Dialkylaminostyryl dyes: specific and highly fluorescent substrates of peroxidase and their application in histochemistry, J. Mol. Histology, 39 (2008) 169-191.
[19] J.W. Schwartz, G. Novarino, D.W. Piston, L.J. DeFelice, Substrate binding stoichiometry and kinetics of the norepinephrine transporter, J. Biol. Chem., 280 (2005) 19177-19184.
[20] J.N. Wilson, A.S. Brown, W.M. Babinchak, C.D. Ridge, J.D. Walls, Fluorescent stilbazolium dyes as probes of the norepinephrine transporter: structural insights into substrate binding, Org. biomol. chem., 10 (2012) 8710-8719.
[21] E.Y. Chernikova, D.V. Berdnikova, Y.V. Fedorov, O.A. Fedorova, F. Maurel, G. Jonusauskas, Light-induced piston nanoengines: ultrafast shuttling of a styryl dye inside cucurbit[7]uril, Phys. Chem. Chem. Phys., 19 (2017) 25834-25839.
[22] S.-H. Li, X. Xu, Y. Zhou, Q. Zhao, Y. Liu, Reversibly Tunable White-Light Emissions of Styrylpyridiniums with Cucurbiturils in Aqueous Solution, Org. Lett., 19 (2017) 6650-6653.
[23] L. Sun, W. Zhu, W. Wang, F. Yang, C. Zhang, S. Wang, X. Zhang, R. Li, H. Dong, W. Hu, Intermolecular Charge-Transfer Interactions Facilitate Two-Photon Absorption in Styrylpyridine-Tetracyanobenzene Cocrystals, Angew. Chem. Int. Ed., 56 (2017) 7831-7835.
[24] E.N. Ushakov, T.P. Martyanov, A.I. Vedernikov, S.N. Sazonov, I.G. Strelnikov, L.S. Klimenko, M.V. Alfimov, S.P. Gromov, Stereospecific [2 + 2]-cross-photocycloaddition in a supramolecular donor-acceptor complex, Tet. Lett., 60 (2019) 150-153.
[25] H. Wu, Y. Chen, X. Dai, P. Li, J.F. Stoddart, Y. Liu, In Situ Photoconversion of Multicolor Luminescence and Pure White Light Emission Based on Carbon Dot-Supported Supramolecular Assembly, J. Am. Chem. Soc., 141 (2019) 6583-6591.
[26] A.K. Vasu, R. Khurana, J. Mohanty, S. Kanvah, pH-responsive molecular assemblies of pyridylbutadiene derivative with cucurbit[7]uril, RSC Adv., 8 (2018) 16738-16745.
[27] A.R. Marri, F.A. Black, J. Mallows, E.A. Gibson, J. Fielden, Pyridinium p-DSSC dyes: An old acceptor learns new tricks, Dyes Pigm., 165 (2019) 508-517.
[28] Y. Ooyama, S. Inoue, T. Nagano, K. Kushimoto, J. Ohshita, I. Imae, K. Komaguchi, Y. Harima, Dye-Sensitized Solar Cells Based On Donor–Acceptor π-Conjugated Fluorescent Dyes with a Pyridine Ring as an Electron-Withdrawing Anchoring Group, Angew. Chem. Int. Ed., 50 (2011) 7429-7433.
[29] M. Cheng, X. Yang, J. Li, C. Chen, J. Zhao, Y. Wang, L. Sun, Dye-Sensitized Solar Cells Based on a Donor–Acceptor System with a Pyridine Cation as an Electron-Withdrawing Anchoring Group, Chem. A Eur.J., 18 (2012) 16196-16202.
[30] J. Cui, J. Lu, X. Xu, K. Cao, Z. Wang, G. Alemu, H. Yuang, Y. Shen, J. Xu, Y. Cheng, Organic sensitizers with pyridine ring anchoring group for p-type dye-sensitized solar cells, J. Phys. Chem. C, 118 (2014) 16433-16440.
[31] Y.V. Faletrov, K.I. Bialevich, I.P. Edimecheva, D.G. Kostsin, E.V. Rudaya, E.I. Slobozhanina, V.M. Shkumatov, 22-NBD-cholesterol as a novel fluorescent substrate for cholesterol-converting oxidoreductases, J. Steroid Biochem. Mol. Biol. 134 (2013) 59-66.
[32] M. Hölttä-Vuori, R.L. Uronen, J. Repakova, E. Salonen, I. Vattulainen, P. Panula, Z. Li, R. Bittman, E. Ikonen, BODIPY-cholesterol: a new tool to visualize sterol trafficking in living cells and organisms, Traffic, 9 (2008) 1839-1849.
[33] J.R. Robalo, J.P.P. Ramalho, L.M.S. Loura, NBD-Labeled Cholesterol Analogues in Phospholipid Bilayers: Insights from Molecular Dynamics, J. Phys.Chem. B, 117 (2013) 13731-13742.

[34] Z. Li, E. Mintzer, R. Bittman, First synthesis of free cholesterol− BODIPY conjugates, J. Org. Chem., 71 (2006) 1718-1721.
[35] C. Almeida, A. De Wreede, A. Lamazière, J. Ayala-Sanmartin, Cholesterol-pyrene as a probe for cholesterol distribution on ordered and disordered membranes: Determination of spectral wavelengths, PloS one, 13 (2018) e0201373.
[36] G. Gimpl, K. Gehrig-Burger, Probes for studying cholesterol binding and cell biology, Steroids, 76 (2011) 216-231.
[37] E. Sezgin, F.B. Can, F. Schneider, M.P. Clausen, S. Galiani, T.A. Stanly, D. Waithe, A. Colaco, A. Honigmann, D. Wüstner, F. Platt, C. Eggeling, A comparative study on fluorescent cholesterol analogs as versatile cellular reporters, J. Lipid Res., 57 (2016) 299-309.
[38] H.M. McBride, M. Neuspiel, S. Wasiak, Mitochondria: More Than Just a Powerhouse, Current Biology, 16 (2006) R551-R560.
[39] S. Wisnovsky, Eric K. Lei, Sae R. Jean, Shana O. Kelley, Mitochondrial Chemical Biology: New Probes Elucidate the Secrets of the Powerhouse of the Cell, Cell Chem. Biol., 23 (2016) 917-927.
[40] X. Liu, L. Yang, Q. Long, D. Weaver, G. Hajnóczky, Choosing proper fluorescent dyes, proteins, and imaging techniques to study mitochondrial dynamics in mammalian cells, Biophys. Rep., 3 (2017) 64-72.
[41] P. Mishra, D.C. Chan, Mitochondrial dynamics and inheritance during cell division, development and disease, Nature Rev. Mol. Cell Biol., 15 (2014) 634.
[42] S.O. Raja, G. Sivaraman, A. Mukherjee, C. Duraisamy, A. Gulyani, Facile Synthesis of Highly Sensitive, Red-Emitting, Fluorogenic Dye for Microviscosity and Mitochondrial Imaging in Embryonic Stem Cells, ChemistrySelect, 2 (2017) 4609-4616.
[43] K. Mebrouk, S. Debnath, M. Fourmigué, F. Camerel, Photothermal Control of the Gelation Properties of Nickel Bis(dithiolene) Metallogelators under Near-Infrared Irradiation, Langmuir, 30 (2014) 8592-8597.
[44] H. Agnihotri, A.K. Vasu, V. Palakollu, S. Kanvah, Neutral and cationic pyridylbutadienes: solvatochromism and fluorescence response with sodium cholate, Photochem. Photobiol. Sci., 14 (2015) 2159-2167.
[45] P. Jana, M. Radhakrishna, S. Khatua, S. Kanvah, A "turn-off" red-emitting fluorophore for nanomolar detection of heparin, Phys. Chem. Chem. Phys., 20 (2018) 13263-13270.
[46] M. Collot, E. Boutant, M. Lehmann, A.S. Klymchenko, BODIPY with Tuned Amphiphilicity as a Fluorogenic Plasma Membrane Probe, Bioconjugate chem., 30 (2019) 192-199.
[47] E. Rideau, R. Dimova, P. Schwille, F.R. Wurm, K. Landfester, Liposomes and polymersomes: a comparative review towards cell mimicking, Chem. Soc. Rev., 47 (2018) 8572-8610.
[48] H.S.P. Rao, A. Desai, J. Sarkar, M. Mohapatra, A.K. Mishra, Photophysical behavior of a new cholesterol attached coumarin derivative and fluorescence spectroscopic studies on its interaction with bile salt systems and lipid bilayer membranes, Phys. Chem. Chem. Phys., 16 (2014) 1247-1256.
[49] L. Plougastel, M.R. Pattanayak, M. Riomet, S. Bregant, A. Sallustrau, M. Nothisen, A. Wagner, D. Audisio, F. Taran, Sydnone-based turn-on fluorogenic probes for no-wash protein labeling and in-cell imaging, Chem. Commun., 55 (2019) 4582-4585.
[50] A.C. Shaikh, M.E. Varma, R.D. Mule, S. Banerjee, P.P. Kulkarni, N.T. Patil, Ionic Pyridinium–Oxazole Dyads: Design, Synthesis, and Application in Mitochondrial Imaging, J. Org. Chem., 84 (2019) 1766-1777.
[51] G. Zhang, Y. Sun, X. He, W. Zhang, M. Tian, R. Feng, R. Zhang, X. Li, L. Guo, X. Yu, S. Zhang, Red-Emitting Mitochondrial Probe with Ultrahigh Signal-to-Noise Ratio Enables High-Fidelity Fluorescent Images in Two-Photon Microscopy, Anal. Chem., 87 (2015) 12088-12095.
[52] Z. Wang, Y. Gu, J. Liu, X. Cheng, J.Z. Sun, A. Qin, B.Z. Tang, A novel pyridinium modified tetraphenylethene: AIE-activity, mechanochromism, DNA detection and mitochondrial imaging, J. Mater. Chem. B, 6 (2018) 1279-1285.

[53] D.C. Chan, Mitochondria: Dynamic Organelles in Disease, Aging, and Development, Cell, 125 (2006) 1241-1252.
[54] Y. Chen, T.W. Rees, L. Ji, H. Chao, Mitochondrial dynamics tracking with iridium(III) complexes, Curr. Opn. Chem. Biol., 43 (2018) 51-57.
[55] V. Soppina, A.K. Rai, A.J. Ramaiya, P. Barak, R. Mallik, Tug-of-war between dissimilar teams of microtubule motors regulates transport and fission of endosomes, Proc. Natl. Acad. Sci., 106 (2009) 19381-19386.
[56] V. Soppina, S.R. Norris, A.S. Dizaji, M. Kortus, S. Veatch, M. Peckham, K.J. Verhey, Dimerization of mammalian kinesin-3 motors results in superprocessive motion, Proc. Natl. Acad. Sci., 111 (2014) 5562-5567.

TOC Graphic

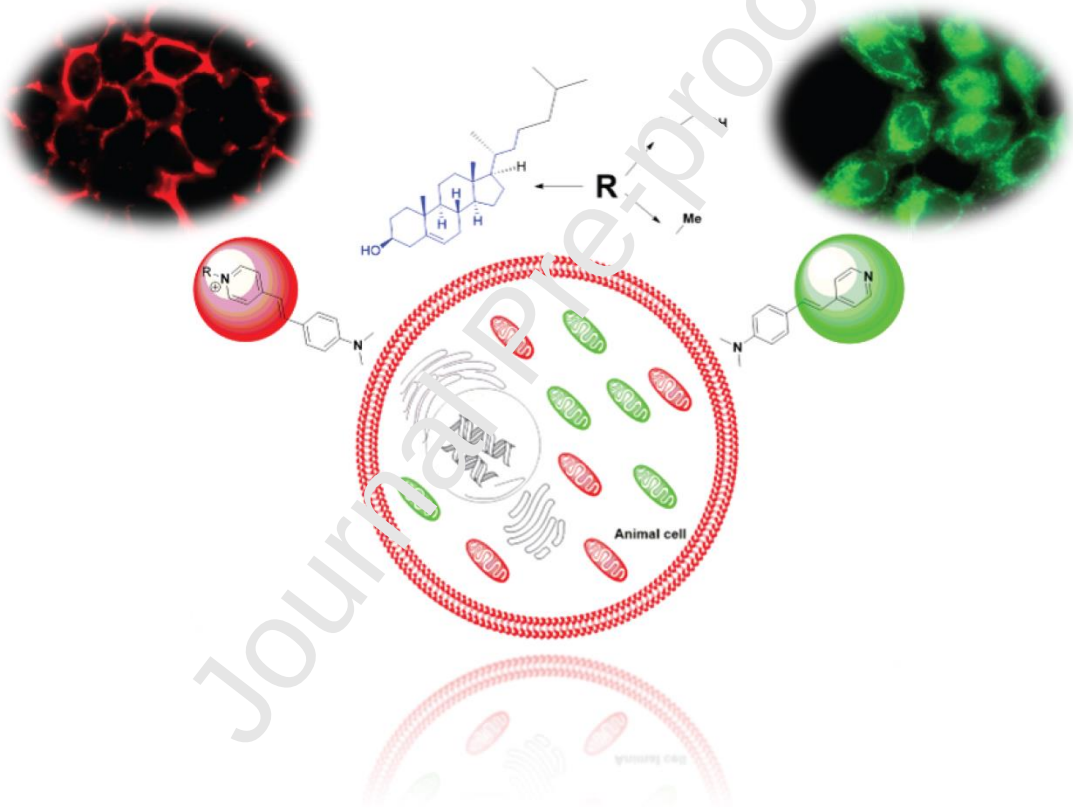

AUTHORSHIP STATEMENT

Manuscript title: **Imaging Mitochondria and Plasma Membrane in Live Cells using Solvatochromic Styrylpyridines**

All authors have contributed to the working of the manuscript.

SK and VS: Supervision, Conceptualization, Methodology, Interpretation, Writing, Reviewing and Editing. **TM**: Synthesis and biological experiments, acquisition of data, analysis and interpretation, Original draft preparation, **AS**: Recombinant DNA tagging for plasmid preparation and acquisition of data, **KB**: Synthesis of molecules and acquisition of data

Declaration of interests

☐ The authors declare that they have no known competing financial interests or personal relationships that could have appeared to influence the work reported in this paper.

☒ The authors declare the following financial interests/personal relationships which may be considered as potential competing interests:

A provisional Indian Patent Application (IP 201921044149) was filed

Imaging Mitochondria and Plasma Membrane in Live Cells using Solvatochromic Styrylpyridines

Tarushyam Mukherjee[‡], Aravintha Siva[†], Komal Bajaj[‡], Virupakshi Soppina*[†] and Sriram Kanvah[‡#]*

[#‡•]Department of Chemistry, Indian Institute of Technology Gandhinagar, Palaj, Gandhinagar 382355, India. E-mail: sriram@iitgn.ac.in, kanvah@gatech.edu

[†•]Department of Biological Engineering, Indian Institute of Technology Gandhinagar Palaj Gandhinagar 382355 e-mail: vsoppina@iitgn.ac.in

Graphical Abstract

- Cholesterol derivatives image plasma membrane and the fluorophores without cholesterol tether image mitochondria

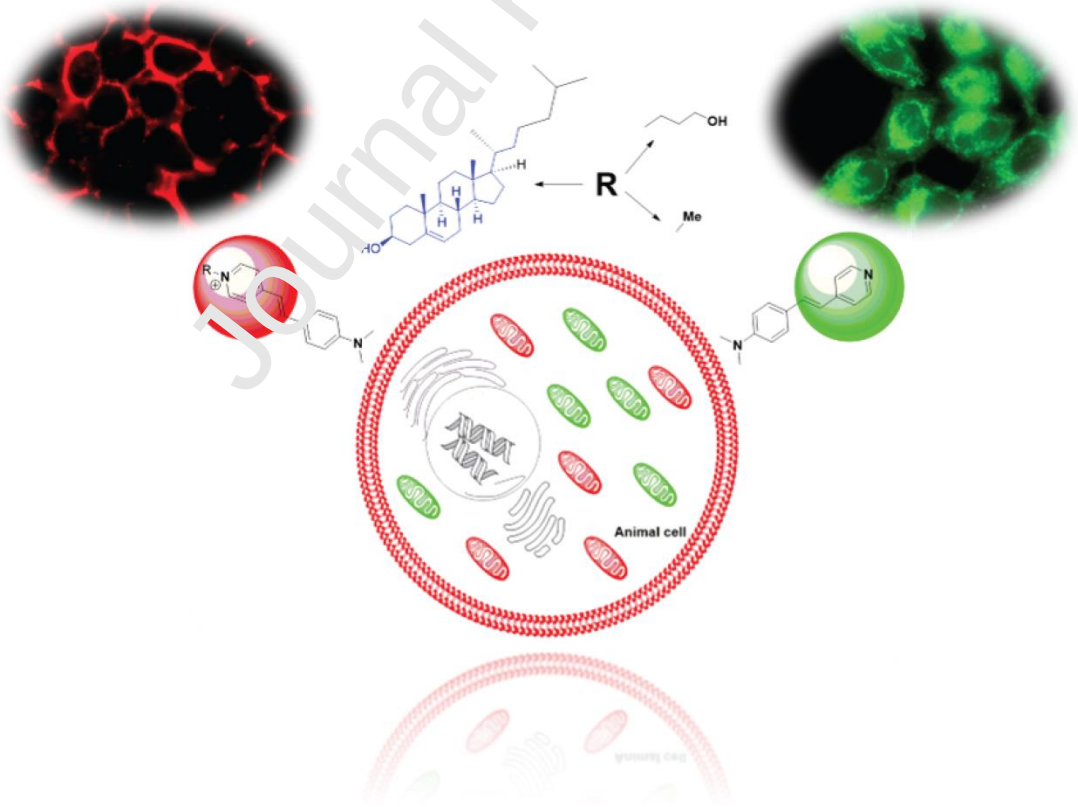

Imaging Mitochondria and Plasma Membrane in Live Cells using Solvatochromic Styrylpyridines

Tarushyam Mukherjee[‡], Aravintha Siva[†], Komal Bajaj[‡], Virupakshi Soppina*[†] and Sriram Kanvah[‡#]*

[#‡•]Department of Chemistry, Indian Institute of Technology Gandhinagar, Palaj, Gandhinagar 382355, India. E-mail: sriram@iitgn.ac.in, kanvah@gatech.edu

[†•]Department of Biological Engineering, Indian Institute of Technology Gandhinagar Palaj Gandhinagar 382355 e-mail: vsoppina@iitgn.ac.in

- Styrlpyridine with and without cholesterol tether were synthesized.
- The fluorophores show solvatochromic emission attributed to intramolecular charge transfer in green to red wavelength regions.
- The neutral and the cationic styrylpyridines image and track mitochondria efficiently and also
- Cholesterol-tethered styrylpyridine stains plasma membrane and also shows robust interaction with liposomes